[1] # Parameter sensitivity and identifiability for a biogeochemical

[2] # model of hypoxia in the northern Gulf of Mexico

[3] **Marcus W. Beck[1], John C. Lehrter[2], Lisa L. Lowe[3]**

[1]*USEPA National Health and Environmental Effects Research Laboratory*
Gulf Ecology Division, 1 Sabine Island Drive, Gulf Breeze, FL 32561
Phone: 850-934-2480, Fax: 850-934-2401
Email: beck.marcus@epa.gov

[2]*Dauphin Island Sea Lab, University of South Alabama*
Dauphin Island, AL 36528
Phone: 251-861-2141 ext. 7567
Email: jlehrter@disl.org

[3]*Lockheed Martin IS & GS - Civil, supporting the USEPA*
Resarch Triangle Park, NC 27709
Phone: 919-541-3985,
Email: lowe.lisa@epa.gov

Version Date: Mon Nov 28 17:05:13 2016 -0600

Abstract

Bio-geo-chemical models are useful tools in environmental sciences that can guide management and policy-making. Consequently, significant time and resources are spent developing these models in system-specific contexts. The optimization of model parameters to maximize precision, including transferability of these models to different systems, are fundamental concerns in the development and application of these tools. This study provides a context for understanding quantitative limitations of coupled hydrodynamic-ecological models by evaluating parameter sensitivity and identifability of a zero-dimensional (0-D) unit of a larger spatio-temporal model of hypoxia on the Louisiana continental shelf of Gulf of Mexico. The analysis provides a contrast of numeric and ecological certainty in parameter subsets using a systematic framework to infer larger trends in dissolved oxygen dynamics over time, having implications for understanding factors that contribute to environmental conditions that are detrimental to aquatic resources. In particular, we focus on issues of parameter identifiability using local sensitivity analyses to provide quantitative descriptions of numerical constraints on model precision. We argue that quantitative and ecological certainty in model calibration are often at odds and practitioners must choose explicit model components to optimize given tradeoffs between the two. We further conclude that numerically optimal parameter sets for models of hypoxia are often small subsets of the complete parameter set because of redundancies in the unique effects of paramater perturbations on model output. As a result, we demonstrate that use of a model for inference into ecological mechanisms of observed or predicted changes in hypoxic condition can be potentially misguided in the absence of quantitative descriptions of identifiability. Although these concerns have been expressed in the literature, they are rarely explicitly addressed or included in model evaluations. In addition to immediate implications for regional models, we provide a framework for describing the effects of parameter uncertainty and identifiability that can be applied to similar models to better inform environmental management.

1 Introduction

Hypoxia formation in bottom waters of coastal oceans occurs primarily from excess nutrient inputs from land-based sources (Justíc et al. 1987, Diaz and Rosenberg 1995, Howarth et al. 1996). These events are detrimental to aquatic organisms and have significant negative effects on economic resources derived from coastal ecosystems (Lipton and Hicks 2003, Diaz and

2

Rosenberg 2011). An understanding of the biological, physical, and chemical processes that contribute to the growth of hypoxic areas is a critical concern for mitigating and preventing these negative impacts. Numerical ecosystem models have been important tools for describing current knowledge of ecosystem processes that contribute to hypoxia formation and for predicting the effects of proposed management activities or future scenarios (Scavia et al. 2004, Hagy and Murrell 2007, Pauer et al. 2016). Unlike statistical models that have more generic structures, simulation and process-based models include explicit descriptions of relevant processes that are constrained by empirical or observational data relevant to the system of interest (e.g. Omlin et al. 2001b, Eldridge and Roelke 2010). These models are often coupled with hydrodynamic grids to provide spatially-explicit representations of patterns in three dimensions (Warner et al. 2005, Zhao et al. 2010, Ganju et al. 2016). Combined hydrodynamic and bio-geo-chemical models have been developed specifically to describe hypoxic conditions on the Louisiana continental shelf (LCS) in the northern Gulf of Mexico (GOM) (Fennel et al. 2013, Obenour et al. 2015, Pauer et al. 2016, Lehrter et al. in review). This area drains a significant portion of the continental United States through the Mississippi-Atchafalaya River Basin (MARB) and is the second largest hypoxic area in the world (Rabalais et al. 2002). Understanding processes that contribute to the frequency and duration of hypoxic events remains a critical research goal for the region, including the application of process-based models to characterize the current knowledge domain.

The development and application of a model represents a tradeoff between characteristics expected from the output or provided by the structural components. An idealized model is sufficiently generalizable across systems, provides results that are precise given the inputs, and includes components that are realistic descriptions of actual processes (Levins 1966). Given that these characteristics cannot be simultaneously achieved, models are developed in partial dependence of reality and theoretical constructs, completely separate from both, or dependent on one or the other (Morrison and Morgan 1999, Ganju et al. 2016). These challenges are analogous to the well-known bias-variance tradeoff in statistical models that balances the competing objectives of over- and under-fitting to an observed dataset. Process-based models are more commonly imbalanced between reality and theory, such that most are over-parameterized in an attempt to completely describe reality (Denman 2003, Nossent and Bauwens 2012, Petrucci and Bonhomme 2014). Such over-parameterization, including use of many structural equations, can

3

have serious implications for practical applications. Quantitative limitations of over-parameterization are analagous to degrees of freedom in standard statistical models as free parameters cannot be numerically estimated when constrained to an observed dataset (Kirchner 2006). More importantly, over-parameterization can limit use across systems outside of the data domain and impose uncertainty in model predictions as realistic values for every variable may not be known or inaccurately applied from existing studies (Durand et al. 2002, Refsgaard et al. 2007, Wade et al. 2008). The application of process-based models to describe hypoxia dynamics has not been immune to these challenges and comprehensive approaches are needed to develop models that more carefully balance theory with reality (e.g., Snowling and Kramer 2001).

Standard approaches for uncertainty analysis can be used to begin addressing model complexity issues. In the most general sense, uncertainty is evaluated relative to the effects of input conditions or the observed data used to calibrate a model, changes in parameter values, or variation in the structural components (Beck 1987). Evaluating parameter uncertainty is by far the most common and simplest means of evaluating model behavior. Although uncertainty analyses should be integrated throughout model development and application, parameters are more often evaluated post-hoc as a form of 'damage control' for further calibration. This approach is sometimes called inverse modelling where results from sensitivity analyses are used to guide calibration or fit of the developed model to observations (Soetaert and Petzoldt 2010, or confronting models with data, *sensu* Hilborn and Mangel 1997). Parameter sensitivity analysis combined with inverse modelling necessarily involves questions of parameter 'identifiability', where only a subset of parameters can be numerically constrained to the data as compared to the entire parameter set. Redundancies in parameter effects lead to unidentifiable models where optimal solutions may be empirically impossible (i.e., standard algorithms will not converge) or parameter values may be non-unique leading to the right answer for the wrong reason (Kirchner 2006). The concept of identifiable parameter subsets is not foreign to hypoxia or eutrophication models (Omlin et al. 2001a, Estrada and Diaz 2010, Mateus and Franz 2015), although there is a clear need for greater integration of these concepts in model development (Fasham et al. 2006). Moreover, the inclusion of sensitivity and identifiability analyses in model tuning will require the adoption of selection rules that are context-dependent given the subsets that are possible with large parameter sets (e.g., Wagener et al. 2001a,b).

This study describes a parameter sensitivity analysis to evaluate identifiability of parameter subsets for a bio-geo-chemical model of hypoxia for the northern GOM. We evaluate a simple zero-dimensional (0-D) unit of a larger spatial-temporal model to explore relationships between multiple parameter sets and hypoxia dynamics on the LCS. Specifically, we provide empirical results to support the assumption that models are generally over-parameterized and only a finite and smaller subset of the larger parameter set can be optimized for a given research question or dataset. We provide explicit guidance for choosing such subsets of the parameter space given constraints on identifiability as directly related to sensitivity analyses. The objectives are to 1) identify the parameters that have the greatest influence on dissolved oxygen (O_2) using local sensitivity analysis, 2) quantify the identifiability of subsets of the total parameter space based on sensitivity, 3) and provide a set of heuristics for choosing parameters based on sensitivity, identifiability, and parameter categories, including extension to other state variables provided by the model. A final analysis evaluates identifiability relative to structural uncertainty to provide an example of extending these methods to more complex uncertainty assessments. The optimum parameter space is defined as the chosen subset that represents the maximum number of identifiable parameters. Here, 'optimum' is both a qualitative description based on a research question or management goal and a quantitative objective based on numerical optimization criteria for fitting model output to a calibration dataset. These results can be used to refine existing models or guide application of models to novel contexts, such as downscaling or application to new environments. We conclude with a discussion of the implications for hypoxia formation in coastal regions, including management strategies for nutrient reduction and use of mechanistic models to inform decision-making.

2 Methods

2.1 Model description

Hypoxic events, defined as <2 mg L^{-1} of O_2 (< 64 mmol m^{-3}), occur seasonally in bottom waters in the northern GOM. The LCS receives high nutrient loads from the MARB that drains a significant portion of the continental United States. Nutrient-stimulated primary production in surface waters increases biological oxygen demand in bottom waters as sinking organic matter is decomposed (Bierman et al. 1994, Murrell et al. 2013). The hypoxic area

averages 15,540 km^2 annually (1993-2015) with minimum concentrations observed from late spring to early fall. Seasonal variation is strongly related to carbon and nutrient export from the MARB (Lohrenz et al. 2008, Bianchi et al. 2010), whereas hydrologic variation, currents, and wind patterns can affect vertical salinity gradients that contribute to the formation of hypoxia (Wiseman et al. 1997, Paerl et al. 1998, Obenour et al. 2015).

This study evaluated the core unit of a recently developed hydrodynamic and ecological model that describes horizontal and vertical transport and mixing of state variables relevant for hypoxia in the northern GOM. The Coastal General Ecosystem Model (CGEM) includes elements from the Navy Coastal Ocean Model (Martin 2000) that describes hydrodynamics on the LCS and a biogeochemical model with multiple plankton groups, water-column metabolism, and sediment diagenesis (Eldridge and Roelke 2010). The hydrodynamic component of CGEM provides a spatially-explicit description of hypoxia using an orthogonal grid with an approximate horizontal resolution of 1.9 km^2 and twenty equally-spaced vertical sigma layers on the shelf (depth $\leq$ 100 m, with additional hybrid layers at deeper depths). The biogeochemical component includes equations for 36 state variables including six phytoplankton groups (with nitrogen and phosophorus quotas for each), two zooplankton groups, nitrate, ammonium, phosphate, dissolved inorganic carbon, oxygen, silica, and multiple variables for dissolved and particulate organic matter from different sources. Atmospheric and hydrological boundary conditions described in Hodur (1997) and Lehrter et al. (2013) are also included in CGEM.

The core unit of CGEM is FishTank, a 0-D model that implements the biogeochemical equations in Eldridge and Roelke (2010) and does not include any form of physical transport (i.e., advection, mixing, or surface flux) nor sediment diagenesis. Although FishTank was developed for specific application in CGEM, it can easily be applied to other hydrodynamic grids. Accordingly, the sensitivity and identifiability analyses described below focused exclusively on FishTank and are informative for both the LCS gridded model as well as potential applications to different systems. The FishTank model provides estimates for the 36 state variables described above using a 0-D parcel that is uniformly mixed as a closed system. A set of initial conditions is provided on execution of the model that is based on observations of relevant variables obtained from research cruises in the northern GOM during April, June, and September of 2006 (Table 1 in Murrell et al. 2014).

154   Results from FishTank are based on time-dependent differential equations that describe
155 energy flow between phytoplankton and zooplankton groups as affected by nutrient uptake rates,
156 organic matter inputs and losses, inherent optical properties, and temperature (Penta et al. 2008,
157 Eldridge and Roelke 2010, see appendix in Lehrter et al. in review). A total of 108 equations are
158 estimated at each time step to return a value for each of the 36 state variables described by the
159 model. In addition to the initial conditions, 251 parameter values for each of the equations are
160 also supplied at model execution. These parameters define relationships among fixed effects in
161 the equations and represent ecological properties described by the model that influence hypoxia
162 formation. Values for each of the parameters were based on estimates from the literature, field or
163 laboratory-based measurements, or expert knowledge in absence of the former. As such, a
164 sensitivity analysis of parameter values is warranted given that, for example, literature or
165 field-based estimates may not apply under all scenarios or expert knowledge is not completely
166 certain (Refsgaard et al. 2007).

167   The sensitivity of O_2 to perturbations of all relevant parameters for the 108 equations was
168 estimated using a five minute timestep of FishTank simulations from January 1st to December
169 31st, 2006. Irrelevant parameters were removed for several reasons; parameters were not relevant
170 for the 0-D model (i.e., hydrodynamic parameters), were considered physical constants, or had no
171 effect given initial conditions. Additionally, FishTank includes six phytoplankton and two
172 zooplankton groups to describe complexity in community structure and foodweb dynamics.
173 However, structural equations for each group are identical such that chosen parameter values
174 primarily control differences between the groups, e.g., large-bodied or small-bodied plankton,
175 slow-growing or fast-growing plankton, etc. Initial analyses indicated that parameter sensitivity of
176 dissolved oxygen was identical within the six phytoplankton and zooplankton groups. To remove
177 obvious redundancies in the model, the sensitivity analyses were conducted using only one
178 phytoplankton and one zooplankton group. The final parameter set that was evaluated included 51
179 parameters that were further grouped into one of six categories based on applicable
180 biogeochemical components of the model: optics ($n = 4$ parameters), organic matter (12),
181 phytoplankton (22), temperature (2), and zooplankton (11). A full description of the model
182 parameters is available as an appendix in Lehrter et al. in review.

2.2 Local sensitivity analysis

The analysis focused on sensitivity of O_2 and other state variables (noted below) in the 0-D FishTank model to identify parameters that may affect spatial and temporal variation of hypoxia in the larger model. A local sensitivity analysis was performed by evaluating the change in O_2 following perturbation of each parameter from its original value. The analyses relied exclusively on concepts used in the FME package developed for the R statistical programming language (Soetaert and Petzoldt 2010, RDCT (R Development Core Team) 2016). Parameters were individually perturbed by 50% of the original values and the model was executed to obtain an estimate O_2 sensitivity. For each perturbation, a sensitivity value S was estimated for each time step i given a change for parameter j as:

$$S_{ij} = \frac{\partial y_i}{\partial \Theta_j} \cdot \frac{w_{\Theta_j}}{w_{y_i}} \tag{1}$$

where the estimate depended on the change in the predicted value for response variable y divided by the change in the parameter Θ_j multiplied by the quotient of scaling factors w for each. The scaling factors, w_{Θ_j} for the parameter Θ_j and w_{y_i} for response variable y_i, were set as the default value of the unperturbed parameter and the predicted value of y_i after perturbation (Soetaert and Petzoldt 2010). The scaling ensures the estimates are unitless such that the relative magnitudes allow comparisons of model sensitivity to parameters and state variables that differ in scale. Sensitivity values for all j parameters were summarized across the time series from $i = 1$ to n as $L1$:

$$L1 = \sum |S_{ij}|/n \tag{2}$$

All parameters for each of the six equation categories (optics, organic matter, phytoplankton, temperature, and zooplankton) that had non-zero $L1$ (suggesting sensitivity) were retained for identifiability analysis.

2.3 Identifiability and selecting parameter subsets

Identifiability of parameter subsets was estimated from the minimum eigenvector of the cross-product of a selected sensitivity matrix (Brun et al. 2001, Omlin et al. 2001a):

$$\gamma = \frac{1}{\sqrt{\min\left(\mathrm{EV}[\hat{S}^{\top}\hat{S}]\right)}} \tag{3}$$

207 where γ ranges from one to infinity for perfectly identifiable (orthogonal) or unidentifiable

208 (perfectly collinear) results for parameters in a sensitivity matrix S. The sensitivity functions

209 were supplied as a matrix $\hat{S}$ with rows i and columns j (eq. (1)) that described deviations of

210 predicted O_2 from the default parameter values. The matrix $\hat{S}$ was first normalized by dividing by

211 the square root of the summed residuals (Omlin et al. 2001a, Soetaert and Petzoldt 2010).

212 The collinearity index γ provides a measure of the linear dependence between sensitivity

213 functions described above for subsets of parameters. Estimates of γ greater than 10-15 suggest

214 parameter sets are poorly identifiable (Brun et al. 2001, Omlin et al. 2001a), meaning parameter

215 values that maximize precision on a calibration dataset are inestimable by conventional

216 optimization algorithms given similar effects of the selected parameters on O_2. Greater sensitivity

217 of a state variable to a subset of parameters does not always imply better identifiability if the

218 individual effects are similar. An intuitive interpretation of γ is provided by Brun et al. (2001)

219 such that a change in a state variable caused by a change in one parameter can be offset by the

220 fraction $1 - 1/\gamma$ by the remaining parameters. That is, $\gamma = 10$ suggests the relative change in O_2

221 for an arbitrary parameter in the selected set can be compensated for by 90% with changes in the

222 other parameters.

223 Initial analyses suggested that considerably limited subsets of parameters were identifiable

224 of the 51 evaluated for the FishTank model. Given this limitation, parameter selection must

225 consider the competing objectives of increased precision with parameter inclusion and reduced

226 identifability as it relates to optimization. An additional challenge is the excessively high number

227 of combinations of parameter sets, which complicates selection given sensitivity differences and

228 desired ecological categories of each parameter (e.g., practicioners may only be interested in

229 optics parameters). For example, Fig. 1 provides a simple graphic of the unique number of

230 combinations that are possible for different subsets of 'complete' parameter sets of different sizes

231 (i.e., based on n choose k combinations equal to $n!/\left(k!\left(n-k\right)!\right)$). The number of unique

232 combinations increases with the total parameters in the set and is also maximized for moderate

233 selections (e.g., selecting half the total). For example, over 10^{14} combinations are possible by

9

selecting 25 parameters from a set of 50. Accordingly, parameter selection is complicated by differing sensitivity, identifiability limits for parameter subsets, and the difficulty of choosing from many combinations.

A set of heuristics was developed that address the tradeoff in model complexity and identifiability given the challenges described above (see also Wagener et al. 2001a). These rulesets were developed with the assumption that parameters will be selected with preference for those with high sensitivity and identifability based on $\gamma < 15$ as an acceptable threshold for subsets (e.g., 93% accountability). Selection heurestics also recognized that parameter categories (i.e., optics, organic matter, phytoplankton, temperature, zooplankton) may have unequal preferences by model users given questions of interest. In all selection scenarios, parameters were selected by decreasing sensitivity starting with the most sensitive until identifiability did not exceed $\gamma = 15$ where selections were 1) blocked within parameter category, 2) independent of parameter category, 3) or considering all categories equally. The selection rules produced seven subsets of parameters that could further be used to optimize model calibration.

2.4   Observational and structural uncertainty

In addition to parameter uncertainty, the effects of observational and structural uncertainty on the sensitivity analyses were evaluated by changing the initial conditions and structural components, respectively, from the default model setup. First, observational uncertainty (i.e., effects of observed data on model output) was evaluated by varying the initial conditions that were based on observational data from research cruises in the northern GOM (Murrell et al. 2014). Uncertainty in these data translates directly to uncertainty that can influence results of the sensitivity analysis. For example, the sensitivity of O_2 to variation in the half-saturation constants for phytoplankton (the concentration supporting half the maximum uptake rate of nutrients) will vary given the initial nutrient concentrations (Eppley et al. 1969). Further, changes in the ratio between nitrogen and phosphorus could affect sensitivity depending on the limiting nutrient. Parameter sensitivity was re-evaluated by varying all initial conditions that were non-zero by different seasonal means based on averages of water quality data across stations and years. April and September seasonal averages of the observed data were used to evaluate the effects of conditions that were typical of spring and late summer on the LCS (Table 1).

The effects of model structure on parameter sensitivity (i.e., structural uncertainty) were

10

evaluated by changing specific components of the model. The FishTank model includes several ecosystem processes or characteristics that can be included based on expected conditions, available data, or desired complexity. These 'switches' are conceptually different from model parameters as they allow the inclusion or exclusion of explicit equations or processes. Switches in FishTank include different structural equations for the vertical attenuation of light through the water column (inherent or apparent optical properties, Penta et al. 2009, Eldridge and Roelke 2010) and chlorophyll to carbon ratio models (fixed or dynamic given light and nutrients, Cloern et al. 1995). Several switches also affect phytoplankton growth including different models for specific growth and effects of temperature, light dependence, nutrient uptake, and internal cell quotas (Lehrter et al. in review, references therein). Parameter sensitivity was evaluated by comparing the results from the default model setup to an alternative, more complex, setup that included additional processes with added switches (Table 2).

2.5 Extension to other state variables

The above analyses were repeated for additional state variables estimated by FishTank to provide further descriptions of ecological dynamics that are relevant for hypoxia. In addition to O_2, other state variables that were evaluated were chlorophyll *a* (chl-*a*), irradiance, nitrate, ammonium, particulate organic matter, dissolved organic matter, and phosphorus. Particulate and dissolved organic matter were estimated as the summation of the respective outputs for organic matter from phytoplankon (*OM1_A*, *OM2_A*) and fecal pellets from zooplankton (*OM1_Z*, *OM2_Z*, see Lehrter et al. in review).

3   Results

4   Discussion

References

Beck MB. 1987. Water quality modeling: A review of the analysis of uncertainty. Water Resources Research, 23(8):1393–1442.

Bianchi TS, DiMarco SF, Jr JHC, Hetland RD, Chapman P, Day JW, Allison MA. 2010. The science of hypoxia in the Northern Gulf of Mexico: a review. Science of the Total Environment, 408(7):1471–1484.

Bierman VJ, Hinz SC, Zhu DW, Wiseman WJ, Rabalais NN, Turner RE. 1994. A preliminary mass-balance model of primary productivity and dissolved oxygen in the Mississippi River plume/ inner Gulf shelf region. Estuaries, 17(4):886–899.

Brun R, Reichert P, Künsch HR. 2001. Practical identifiability analysis of large environmental simulation models. Water Resources Research, 37(4):1015–1030.

Cloern JE, Grenz C, Vidergar-Lucas L. 1995. An empirical model of the phytoplankton:carbon ratio - the conversion factor between productivity and growth rate. Limnology and Oceanography, 40(7):1313–1321.

Denman KL. 2003. Modelling planktonic ecosystems: parameterizing complexity. Progress in Oceanography, 57(3-4):429–452.

Diaz RJ, Rosenberg R. 1995. Marine benthic hypoxia: A review of its ecological effects and the behavioural responses of benthic macrofauna. Oceanography and Marine Biology, 33:245–303.

Diaz RJ, Rosenberg R. 2011. Introduction to environmental and economic consequences of hypoxia. International Journal of Water Resources Development, 27(1):71–82.

Durand P, Gascuel-Odoux C, Cordier MO. 2002. Parameterisation of hydrological models: a review and lessons learned from studies of an agricultural catchment (Naisin, France. Agronomie, 22(2):217–228.

Eldridge PM, Roelke DL. 2010. Origins and scales of hypoxia on the Louisiana shelf: importance of seasonal plankton dynamics and river nutrients and discharge. Ecological Modelling, 221(7):1028–1042.

Eppley RW, Rogers JN, McCarthy J. 1969. Half-saturation constants for uptake of nitrate and ammonium by marine phytoplankton. Limnology and Oceanography, 14(6):912–920.

Estrada V, Diaz M. 2010. Global sensitivity analysis in the development of first principle-based eutrophication models. Environmental Modelling and Software, 25:1539–1551.

Fasham MJR, Flynn KJ, Pondaven P, Anderson TR, Boyd PW. 2006. Development of a robust marine ecosystem model to predict the role of iron in biogeochemical cycles: A comparison of results for iron-replete and iron-limited areas, and the SOIREE iron-enrichment experiment. Deep-Sea Research I, 53:333–366.

Fennel K, Hu J, Laurent A, Marta-Almeida M, Hetland R. 2013. Sensitivity of hypoxia predictions for the northern Gulf of Mexico to sediment oxygen consumption and model nesting. Journal of Geophysical Research: Oceans, 118(2):990–1002.

Ganju NK, Brush MJ, Rashleigh B, Aretxabaleta AL, del Barrio P, Grear JS, Harris LA, Lake SJ, McCardell G, O'Donnell J, Ralston DK, Signell RP, Testa JM, Vaudrey JMP. 2016. Progress and challenges in coupled hydrodynamic-ecological estuarine modeling. Estuaries and Coasts, 39(2):311–332.

Hagy JD, Murrell MC. 2007. Susceptibility of a northern Gulf of Mexico estuary to hypoxia: An analysis using box models. Estuarine Coastal and Shelf Science, 74:239–253.

Hilborn R, Mangel M. 1997. The Ecological Detective: Confronting Models with Data. Princeton University Press, Princeton, New Jersey.

Hodur RM. 1997. The Naval Research Laboratory's Coupled Ocean/Atmosphere Mesoscale Prediction System (COAMPS). Monthly Weather Review, 125:1414–1430.

Howarth RW, Billen G, Swaney D, Townsend A, Jaworski N, Lajtha K, Downing JA, Elmgren R, Caraco N, Jordan T, Berendse F, Freney J, Kudeyarov V, Murdoch P, Zhao-Liang Z. 1996. Regional nitrogen budgets and riverine N & P fluxes for the drainages to the North Atlantic Ocean: natural and human influences. Biogeochemistry, 35(1):75–139.

Justíc D, Legovíc T, Rottini-Sandrini L. 1987. Trends in oxygen content 1911–1984 and occurrence of benthic mortality in the northern Adriatic Sea. Estuarine, Coastal and Shelf Science, 25(4):435–445.

Kirchner JW. 2006. Getting the right answers for the right reasons: Linking measurements, analyses, and models to advance the science of hydrology. Water Resources Research, 42(3):W03S04.

Lehrter JC, Ko DS, Lowe L, Penta B. In review. Predicted effects of climate change on the severity of northern Gulf of Mexico hypoxia. In: Justic et al., editor, Modeling Coastal Hypoxia: Numerical Simulations of Patterns, Controls, and Effect of Dissolved Oxygen Dynamics. Springer, New York.

Lehrter JC, Ko DS, Murrell MC, III JDH, Schaeffer BA, Greene RM, Gould RW, Penta B. 2013. Nutrient distributions, transports, and budgets on the inner margin of a river-dominated continental shelf. Journal of Geophysical Research, 118(10):4822–4838.

Levins R. 1966. The strategy of model building in population biology. American Scientist, 54(4):421–431.

Lipton D, Hicks R. 2003. The cost of stress: low dissolved oxygen and eocnomic benefits of recreational striped bass (*Morone saxatilis* fishing in the Patuxent River. Estuaries, 26(2A):310–315.

355 Lohrenz SE, Redalje DG, Cai WJ, Acker J, Dagg M. 2008. A retrospective analysis of nutrients
356   and phytoplankton productivity in the Mississippi River plume. Continental Shelf Research,
357   28(12):1466–1475.

358 Martin PJ. 2000. Description of the navy coastal ocean model version 1.0. Technical Report
359   NRL/FR/7322-00-9962, Naval Research Lab, Stennis Space Center, Mississippi.

360 Mateus MD, Franz G. 2015. Sensitivity analysis in a complex marine ecological model. Water,
361   7:2060–2081.

362 Morrison M, Morgan MS. 1999. Models as mediating agents. In: Morgan MS, Morrison M,
363   editors, Models as Mediators, page 401. Cambridge University Press, Cambridge.

364 Murrell MC, Beddick DL, Devereux R, Greene RM, III JDH, Jarvis BM, Kurtz JC, Lehrter JC,
365   Yates DF. 2014. Gulf of mexico hypoxia research program data report: 2002-2007. Technical
366   Report EPA/600/R-13/257, US Environmental Protection Agency, Washington, DC.

367 Murrell MC, Stanley RS, Lehrter JC, Hagy JD. 2013. Plankton community respiration, net
368   ecosystem metabolism, and oxygen dynamics on the Louisiana continental shelf: Implications
369   for hypoxia. Continental Shelf Research, 52:27–38.

370 Nossent J, Bauwens W. 2012. Multi-variable sensitivity and identifiability analysis for a complex
371   environmental model in view of integrated water quantity and water quality modeling. Water
372   Science & Technology, 65(3):539–549.

373 Obenour DR, Michalak AM, Scavia D. 2015. Assessing biophysical controls on Gulf of Mexico
374   hypoxia through probabilistic modeling. Ecological Applications, 25(2):492–505.

375 Omlin M, Brun R, Reichert P. 2001a. Biogeochemical model of Lake Zürich: sensitivity,
376   identifiability and uncertainty analysis. Ecological Modelling, 141(1-3):105–123.

377 Omlin M, Reichert P, Forster R. 2001b. Biogeochemical model of Lake Zürich: model equations
378   and results. Ecological Modelling, 141(1-3):77–103.

379 Paerl HW, Pinckney JL, Fear JM, Peierls BL. 1998. Ecosystem responses to internal and
380   watershed organic matter loading: consequences for hypoxia in the eutrophying Neuse River
381   Estuary, North Carolina, USA. Marine Ecology Progress Series, 166:17–25.

382 Pauer JJ, Feist TJ, Anstead AM, DePetro PA, Melendez W, Lehrter JC, Murrell MC, Zhang X, Ko
383   DS. 2016. A modeling study examining the impact of nutrient boundaries on primary
384   production on the Louisiana continental shelf. Ecological Modelling, 328:136–147.

385 Penta B, Lee Z, Kudela RM, Palacios SL, Gray DJ, Jolliff JK, Shulman IG. 2008. An underwater
386   light attenuation scheme for marine ecosystem models. Optical Express, 16(21):16581–16591.

387 Penta B, Lee Z, Kudela RM, Palacios SL, Gray DJ, Jolliff JK, Shulman IG. 2009. An underwater
388   light attenuation scheme for marine ecosystem models: errata. Optical Express,
389   17(25):23351–23351.

Petrucci G, Bonhomme C. 2014. The dilemma of spatial representation for urban hydrology semi-distributed modelling: trade-offs among complexity, calibration and geographical data. Journal of Hydrology, 517:997–1007.

Rabalais NN, Turner RE, Scavia D. 2002. Beyond science into policy: Gulf of Mexico hypoxia and the Mississippi river. BioScience, 52(2):129–142.

RDCT (R Development Core Team). 2016. R: A language and environment for statistical computing, v3.3.1. R Foundation for Statistical Computing, Vienna, Austria. http://www.R-project.org.

Refsgaard JC, van der Sluijs JP, Højberg AL, Vanrolleghem PA. 2007. Uncertainty in the environmental modelling process - a framework and guidance. Environmental Modelling & Software, 22(11):1543–1556.

Scavia D, Justic D, Bierman VJ. 2004. Reducing hypoxia in the Gulf of Mexico: Advice from three models. Estuaries, 27(3):419–425.

Snowling SD, Kramer JR. 2001. Evaluating modelling uncertainty for model selection. Ecological Modelling, 138:17–30.

Soetaert K, Petzoldt T. 2010. Inverse modelling, sensitivity, and Monte Carlo analysis in R using package FME. Journal of Statistical Software, 33(3):1–28.

Wade AJ, Jackson BM, Butterfield D. 2008. Over-parameterised, uncertain 'mathematical marionettes' - how can we best use catchment water quality models? An example of an 80-year catchment-scale nutrient balance. Science of the Total Environment, 400(1-3):52–74.

Wagener T, Boyle DP, Lees MJ, Wheater HS, Gupta HV, Sorooshian S. 2001a. A framework for development and application of hydrological models. Hydrology and Earth System Sciences, 5(1):13–26.

Wagener T, Lees MJ, Wheater HS. 2001b. A toolkit for the development and application of parsimonious hydrological models. In: Singh VP, Meyer DKFSP, editors, Mathematical Models of Small Watershed Hydrology and Applications - Volume 2, pages 91–140. Water Resources Publications LLC, USA.

Warner JC, Geyer WR, Lerczak JA. 2005. Numerical modeling of an estuary: a comprehensive skill assessment. Journal of Geophysical Research: Oceans, 110(C5):13.

Wiseman WJ, Rabalais NN, Turner RE, Dinnel SP, MacNaughton A. 1997. Seasonal and interannual variability within the Louisiana coastal current: stratification and hypoxia. Journal of Marine Systems, 12(1-4):237–248.

Zhao L, Chen C, Vallino J, Hopkinson C, Beardsley RC, Lin H, Lerczak J. 2010. Wetland-estuarine-shelf interactions on the Plum Island Sound and Merrimack River in the Massachusetts coast. Journal of Geophysical Research, 115(C10):13.

Table 1: Initial conditions that were varied to evaluate effects of observational uncertainty on parameter sensitivity. April and September values are based on seasonal averages from water quality samples of the LCS. All units are μmol L^{-1}.

Variables	Default	April	September
Dissolved Inorganic Carbon	2134	2096.5	2133.37
Ammonium	1.09	1.79	0.35
Nitrate	71.4	3.75	2.04
Dissolved Oygen	172	194.47	152.57
Phosphate	1.81	0.23	0.42
Silica	71.4	5.84	9.77

Table 2: Model switches that were used to evaluate effects of structural uncertainty on parameter sensitivity.

Switch type	Default	Complex
Temperature	sigmoidal	Arrenhius
Uptake	Michaelis-Menten	Geider
Quota	Droop	Flynn
Chla:C	regression	Cloern
Photosynthesis	photoinhibition	nutrient dependent
Growth	minimum	*umax* is nutrient dependent

16

Table 3: Sensitivity of O_2 to perturbations of individual parameters. Sensitivities are based on a 50% increase from the initial parameter value, where $L1$ summarizes differences in model output from the default (see eq. (2)). Parameters that did not affect O_2 are not shown. Parameters are grouped by categories as optics, temperature, phytoplankton, zooplankton, and organic matter.

Description	Parameter	L1
Optics		
Chla specific absorption at 490 nm	*astar490*	7.51×10^{-4}
OMZ specific absorption at 490 nm	*astarOMZ*	4.92×10^{-5}
OMA specific absorption at 490 nm	*astarOMA*	4.39×10^{-5}
Temperature		
Optimum temperature for growth(C)	*Tref(nospA+nospZ)$_{p1}$*	0.02
Phytoplankton		
maximum growth rate	*umax*	0.05
mortality coefficient	*mA*	0.02
initial slope of the photosynthesis-irradiance relationship	*alpha*	0.02
edibility vector for Z1	*ediblevector(Z1)*	0.02
phytoplankton carbon/cell	*Qc*	0.01
phytoplankton growth respiration coefficient	*respg*	8.36×10^{-3}
N-uptake rate measured at umax	*vmaxN*	8.12×10^{-3}
phytoplankton basal respiration coefficient	*respb*	6.94×10^{-3}
Phytoplankton threshold for grazing, is multiplied by VOLcell	*Athresh*	4.57×10^{-3}
minimum N cell-quota	*QminN*	4.32×10^{-3}
P-uptake rate measured at umax	*vmaxP*	4.27×10^{-3}
coefficient for non-limiting nutrient	*aN*	4.23×10^{-3}
phytoplankton volume/cell	*volcell*	4.13×10^{-3}
half-saturation constant for P	*Kp*	2.9×10^{-3}
half-saturation constant for N	*Kn*	2.77×10^{-4}
minimum P cell-quota	*QminP*	8.34×10^{-8}
Zooplankton		
half saturation coefficient for grazing	*ZKa*	0.05
zooplankton nitrogen/individual	*ZQn*	0.02
Zooplankton mortality constant for quadratic mortality	*Zm*	0.02
maximum growth rate of zooplankton	*Zumax*	0.02
assimilation efficiency as a fraction of ingestion	*Zeffic*	0.01
proportion of grazed phytoplankton lost to sloppy feeding	*Zslop*	7.78×10^{-3}
Zooplankton growth-dependent respiration factor	*Zrespg*	5.32×10^{-3}
Zooplankton biomass-dependent respiration factor	*Zrespb*	2.96×10^{-3}
zooplankton carbon/individual	*ZQc*	9.38×10^{-5}
zooplankton phosphorus/individual	*ZQp*	3.69×10^{-5}
Organic Matter		
turnover rate for OM1A and OM1Z	*KG1*	6.15×10^{-3}
turnover rate for OM2A and OM2Z	*KG2*	3.14×10^{-3}
O2 concentration that inhibits denitrification	*KstarO2*	3.04×10^{-3}
decay rate of CDOM, 1/day	*KGcdom*	2.98×10^{-3}
half-saturation concentration for O2 utilization	*KO2*	5.85×10^{-4}
half-saturation concentration for NO3 used in denitrification	*KNO3*	5.8×10^{-4}
maximum rate of nitrification per day	*nitmax*	4.99×10^{-4}
NH4 rate constant for nitrification	*KNH4*	4.17×10^{-4}

*Temperature parameters apply separately to phytoplankton ($p1$, one group) or zooplankton ($z1$, one group), denoted by subscripts

Table 4: Parameter identifiability (as γ, eq. (3)) by category for relevant state variables. Selections followed the first heuristic where parameters were selected within categories from most to least sensitive until $\gamma > 15$. Rank describes the relative parameter sensitivity in each category for each state variable.

Parameter	Rank	Ammonium	Chl-a	O$_2$	Irradiance	Nitrate	OM1	OM2	Phosphate
Phytoplankton									
alpha	3	-	-	1.44	1.98	-	-	-	-
alpha	4	3.55	4.57	-	-	-	-	-	-
alpha	5	-	-	-	-	-	10.11	-	-
astar490	1	1	1	1	1	1	1	1	1
astarOMA	2	7.33	5.42	-	5.36	-	7.78	7.87	-
Optics									
astarOMA	3	-	-	3.87	-	-	-	-	10.04
astarOMZ	2	-	-	1.39	-	-	-	-	4.73
astarOMZ	3	7.58	5.51	-	6.02	-	7.91	7.87	-
Athresh	6	11.27	-	-	-	-	-	-	-
ediblevector(Z1)	2	1.13	1.17	-	-	-	1.15	-	-
ediblevector(Z1)	3	-	-	-	-	-	-	2.9	-
ediblevector(Z1)	4	-	-	2.09	4.09	-	-	-	-
KG1	1	-	-	1	-	-	1	-	1
KG1	2	-	1.12	-	1.93	-	-	-	-
KG1	3	4.09	-	-	-	-	-	-	-
KG2	1	-	-	-	-	-	-	1	-
KG2	2	-	-	6	-	-	-	-	13.43
KG2	3	-	-	-	8.19	-	-	-	-
KGcdom	1	-	1	-	1	-	-	-	-
KGcdom	2	-	-	-	-	-	1.47	1.39	-
KGcdom	3	-	-	-	-	-	-	-	13.75
KGcdom	4	4.19	-	6.12	-	-	-	-	-
KNH4	2	4.03	-	-	-	-	-	-	-
Organic Matter									
KO2	3	-	-	-	-	-	14.07	11.96	-
KO2	4	-	-	-	-	-	-	-	14.68
KO2	5	9.47	-	8.61	-	-	-	-	-
KstarO2	1	-	-	-	-	1	-	-	-
KstarO2	3	-	-	6.04	-	-	-	-	-
KstarO2	4	-	-	-	10.65	-	14.08	-	-
mA	1	1	1	-	-	-	1	1	-
mA	2	-	-	1.19	1.29	-	-	-	-
nitmax	1	1	-	-	-	-	-	-	-
Qc	2	-	-	-	-	11.57	-	-	-
Qc	4	-	-	-	-	-	4.98	-	-
Qc	5	-	-	2.9	-	-	-	-	-
respg	6	-	-	3.41	-	-	-	-	-
umax	1	-	-	1	1	1	-	-	1
umax	2	-	-	-	-	-	-	1.21	-
umax	3	2.73	2.11	-	-	-	3.26	-	-
vmaxN	4	-	-	-	-	-	-	4.9	-
vmaxN	5	8.14	-	-	-	-	-	-	-
vmaxN	7	-	-	3.97	-	-	-	-	-
vmaxP	2	-	-	-	-	-	-	-	7.45
Zooplankton									
ZKa	1	-	-	1	1	1	-	-	1
ZKa	2	-	4.31	-	-	-	7.3	5.43	-
Zm	3	-	-	4.57	-	-	-	-	-
Zm	4	-	-	-	11.86	-	-	-	-
ZQn	2	-	-	3.18	6.32	9.76	-	-	8.54
Zumax	1	1	1	-	-	-	1	1	-
Zumax	3	-	-	-	6.93	-	-	-	-
Zumax	4	-	-	5.2	-	-	-	-	-

Table 5: Parameter identifiability (as γ, eq. (3)) for relevant state variables. Selections followed the second heuristic where parameters were selected independent of category from most to least sensitive (L1, eq. (2)), until $\gamma > 15$. Rank describes the relative parameter sensitivity in each category for each state variable (O: optics, OM: organic matter, P: phytoplankton, T: temperature, Z: zooplankton). See Fig. 6 for a graphical illustration.

Selections by state variable	Parameter	L1	Rank	γ
Ammonium				
1	mA	8.49	1_P	1
2	$nitmax$	1.54	1_{OM}	1.16
3	$Zumax$	1.42	1_Z	2.9
Chlorophyll				
1	mA	13.94	1_P	1
2	$Zumax$	1.02	1_Z	1.18
Dissolved Oxygen				
1	$umax$	0.05	1_P	1
2	ZKa	0.05	1_Z	2.17
3	mA	0.02	2_P	2.31
4	$Tref(nospA+nospZ)_{p1}$	0.02	1_T	2.37
5	ZQn	0.02	2_Z	4.69
6	$alpha$	0.02	3_P	4.91
7	Zm	0.02	3_Z	6.73
8	$Zumax$	0.02	4_Z	6.81
Irradiance				
1	ZKa	0.13	1_Z	1
2	$umax$	0.09	1_P	4.41
3	ZQn	0.06	2_Z	7.54
4	mA	0.05	2_P	8.17
5	$KGcdom$	0.05	1_{OM}	9.44
6	$alpha$	0.04	3_P	9.66
7	$Zumax$	0.04	3_Z	10.79
Nitrate				
1	$umax$	8.49	1_P	1
OM1				
1	mA	7.22	1_P	1
2	$Zumax$	0.96	1_Z	1.15
3	$KG1$	0.92	1_{OM}	3.87
OM2				
1	mA	14.25	1_P	1
2	$Tref(nospA+nospZ)_{p1}$	1.48	1_T	1.05
3	$umax$	1.11	2_P	2.46
4	$Zumax$	1.01	1_Z	2.91
Phosphate				
1	ZKa	1.47	1_Z	1
2	$umax$	0.78	1_P	11.45
3	$vmaxP$	0.59	2_P	11.48
4	ZQn	0.5	2_Z	13.74

Table 6: Parameter identifiability (as γ, eq. (3)) for relevant state variables. Selections followed the third heuristic where parameters were selected equally within each category from most to least sensitive (L1, eq. (2)), until $\gamma > 15$. Rank describes the relative parameter sensitivity in each category for each state variable (O: optics, OM: organic matter, P: phytoplankton, T: temperature, Z: zooplankton).

Selections by state variable	Parameter	L1	Rank	γ
Ammonium				
1	*mA*	8.49	1_P	1
2	*nitmax*	1.54	1_{OM}	1.16
3	*Zumax*	1.42	1_Z	2.9
4	*Tref(nospA+nospZ)$_{p1}$*	0.79	1_T	3.46
5	*astar490*	0.03	1_O	4.25
Chlorophyll				
1	*mA*	13.94	1_P	1
2	*Zumax*	1.02	1_Z	1.18
3	*Tref(nospA+nospZ)$_{p1}$*	0.6	1_T	2.62
4	*KGcdom*	0.07	1_{OM}	3.24
5	*astar490*	0.02	1_O	5.98
Dissolved Oxygen				
1	*umax*	0.05	1_P	1
2	*ZKa*	0.05	1_Z	2.17
3	*Tref(nospA+nospZ)$_{p1}$*	0.02	1_T	2.29
4	*KG1*	0.01	1_{OM}	3.85
5	*astar490*	7.51×10^{-4}	1_O	3.89
6	*mA*	0.02	2_P	4.42
7	*ZQn*	0.02	2_Z	5.22
Irradiance				
1	*ZKa*	0.13	1_Z	1
2	*umax*	0.09	1_P	4.41
3	*KGcdom*	0.05	1_{OM}	4.5
4	*Tref(nospA+nospZ)$_{p1}$*	0.03	1_T	4.5
5	*astar490*	0.02	1_O	6.9
6	*ZQn*	0.06	2_Z	10.63
7	*mA*	0.05	2_P	11.21
8	*KG1*	0	2_{OM}	14.65
9	*astarOMA*	0	2_O	14.72
Nitrate				
1	*umax*	8.49	1_P	1
OM1				
1	*mA*	7.22	1_P	1
2	*Zumax*	0.96	1_Z	1.15
3	*KG1*	0.92	1_{OM}	3.87
4	*Tref(nospA+nospZ)$_{p1}$*	0.86	1_T	3.93
5	*astar490*	0.03	1_O	5.81
OM2				
1	*mA*	14.25	1_P	1
2	*Tref(nospA+nospZ)$_{p1}$*	1.48	1_T	1.05
3	*Zumax*	1.01	1_Z	2.61
4	*KG2*	0.94	1_{OM}	3.39
5	*astar490*	0.04	1_O	4.46
6	*umax*	1.11	2_P	6.02
7	*ZKa*	0.88	2_Z	9.21
Phosphate				
1	*ZKa*	1.47	1_Z	1
2	*umax*	0.78	1_P	11.45
3	*Tref(nospA+nospZ)$_{p1}$*	0.16	1_T	13.71
4	*KG1*	0.14	1_{OM}	14.64

Table 7: Changes in mean sensitivity of state variables by parameter categories to different initial conditions and structural components of the model. Changes show the difference in average sensitivity from results using the default model setup. Sensitivities are based on average $L1$ (see eq. (2)) values of the state variables to changes in parameters in each parameter category. Increases in average sensitivity are in bold. Medians and ranges of sensitivity values for the different conditions are shown in Fig. 7.

| State variables by parameter category		Change		
	Default sensitivity	Initial: April	Initial: September	Structure: complex
Optics				
Ammonium	0.01	**0.01**	**0.01**	**0.01**
Chlorophyll	0.01	**0.01**	**0.01**	**0.01**
Dissolved Oxygen	2.81×10^{-4}	$\mathbf{2.11 \times 10^{-4}}$	$\mathbf{1.46 \times 10^{-4}}$	$\mathbf{1.93 \times 10^{-4}}$
Irradiance	0.01	-0	-0	-0
Nitrate	0.01	**0.01**	**0.01**	**0.01**
OM1	0.01	**0.01**	**0.01**	**0.01**
OM2	0.02	**0.01**	**0.01**	**0.01**
Phosphate	0	**0**	**0**	**0**
Organic Matter				
Ammonium	0.31	-0.08	-0.04	$\mathbf{2.22 \times 10^{-4}}$
Chlorophyll	0.02	-0.12	-0.14	**0.01**
Dissolved Oxygen	0	$\mathbf{6.75 \times 10^{-4}}$	-2.32×10^{-4}	**0**
Irradiance	0.01	-0.01	-0.01	$\mathbf{2.99 \times 10^{-4}}$
Nitrate	0.12	-0.06	-0.09	**0.1**
OM1	0.13	-0.15	-0.12	-0.04
OM2	0.14	-0.07	-0.17	-0.05
Phosphate	0.03	-0.04	-0.06	**0.02**
Phytoplankton				
Ammonium	0.8	**0.02**	-0.3	-65.98
Chlorophyll	1.14	-1.23	-4.38	-104.24
Dissolved Oxygen	0.01	$\mathbf{4.58 \times 10^{-4}}$	-0	-3.44×10^{-4}
Irradiance	0.02	**0**	-0	-0.01
Nitrate	0.74	**0.43**	**0.45**	**0.64**
OM1	0.76	-0.17	-0.46	-55.11
OM2	1.28	-0.34	-1.15	-128.93
Phosphate	0.17	-0.03	-0.05	**0.14**
Temperature				
Ammonium	0.79	**0.69**	**0.69**	-272.31
Chlorophyll	0.6	**0.47**	**0.45**	-114.51
Dissolved Oxygen	0.02	**0.02**	**0.02**	**0.01**
Irradiance	0.03	**0.02**	**0.02**	-0.01
Nitrate	0.3	**0.15**	**0.16**	**0.19**
OM1	0.86	**0.68**	**0.69**	-215.17
OM2	1.48	**1.21**	**1.2**	-900.26
Phosphate	0.16	**0.11**	**0.09**	**0.11**
Zooplankton				
Ammonium	0.47	**0.45**	**0.44**	**0.16**
Chlorophyll	0.39	**0.26**	**0.23**	**0.2**
Dissolved Oxygen	0.01	**0.01**	**0.01**	**0.01**
Irradiance	0.03	**0.02**	**0.02**	**0.01**
Nitrate	1.06	**1.02**	**1.02**	**0.98**
OM1	0.37	**0.27**	**0.28**	**0.18**
OM2	0.39	**0.3**	**0.28**	**0.18**
Phosphate	0.31	**0.19**	**0.17**	**0.27**
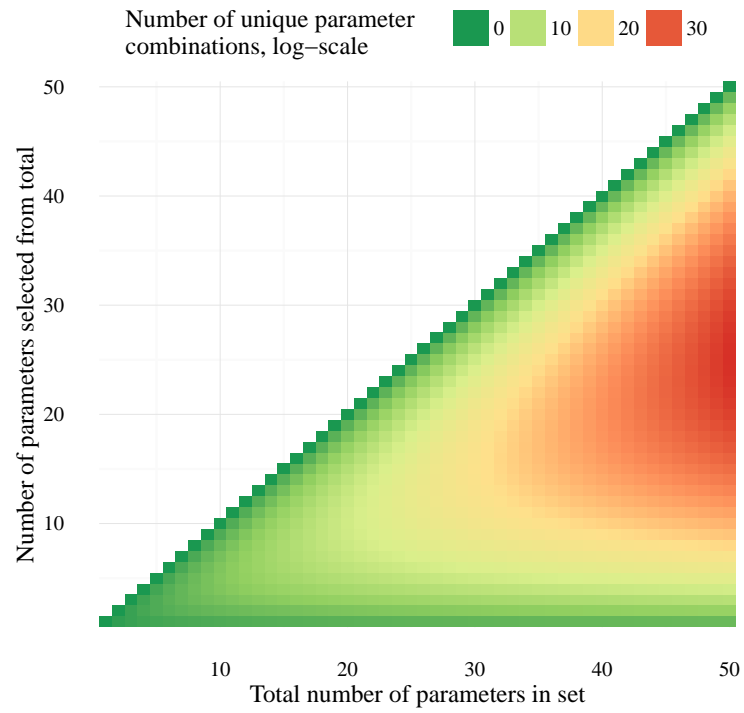
Fig. 1: Examples of unique parameter combinations from different parameter sets and number of selected parameters. The number of combinations are shown for increasing numbers of selected parameters from the total in the set, where 50 parameter sets are shown each with one through 50 total parameters. Note that the number of unique combinations is shown as the natural-log.
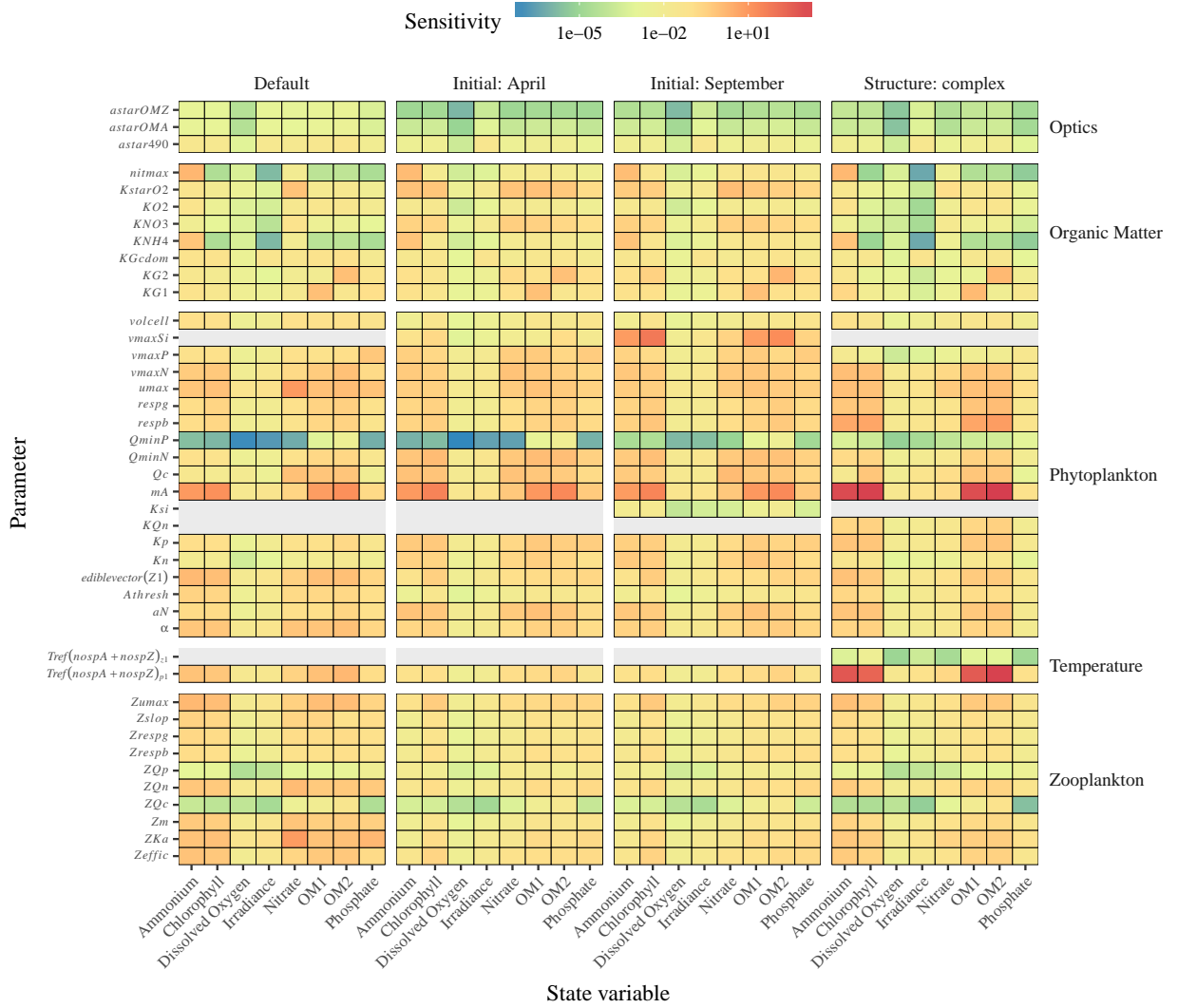
Fig. 2: Sensitivity values (L1, eq. (2)) of all state variables to changes in parameter values using default conditions, changes in initial conditions (April, September seasonal means, Table 1), and changes in structural complexity (Table 2). Parameters are grouped by category: optics, organic matter, phytoplankton, zooplankton, temperature, and zoplankton. See Table 3 for L1 values for O_2 and Tables S1 to S7 for the other state variables.
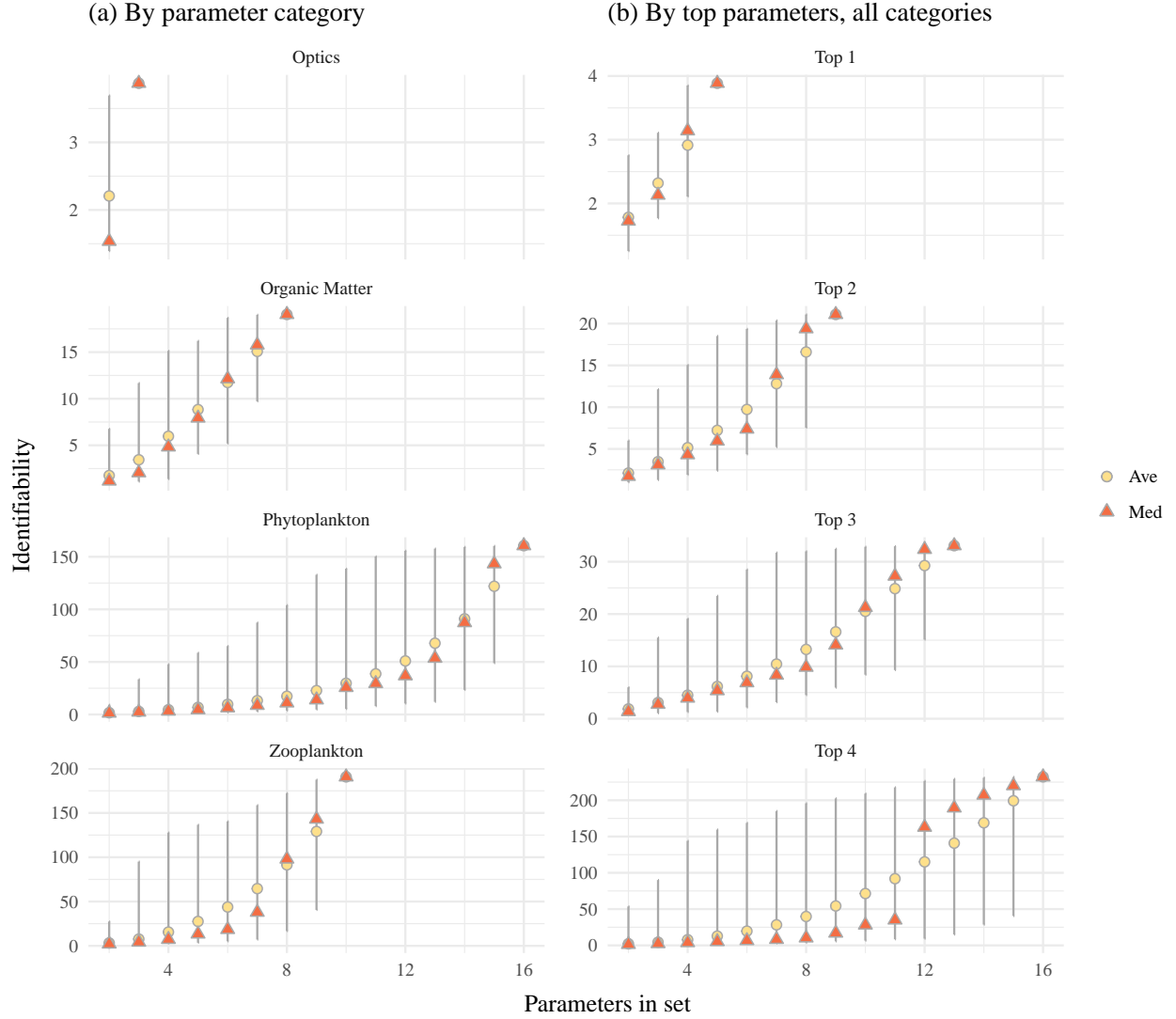
Fig. 3: Identifiability (as γ, eq. (3)) of parameter subsets for O_2. Plots in (a) show identifiability by parameter categories and (b) shows identifiability by selecting the top 1 through 4 parameters in all categories. Lines represent identifiability ranges for the possible combinations given the number of parameters in the set. The temperature category is not shown because O_2 was sensitive to only one parameter (i.e., $\gamma = 1$).
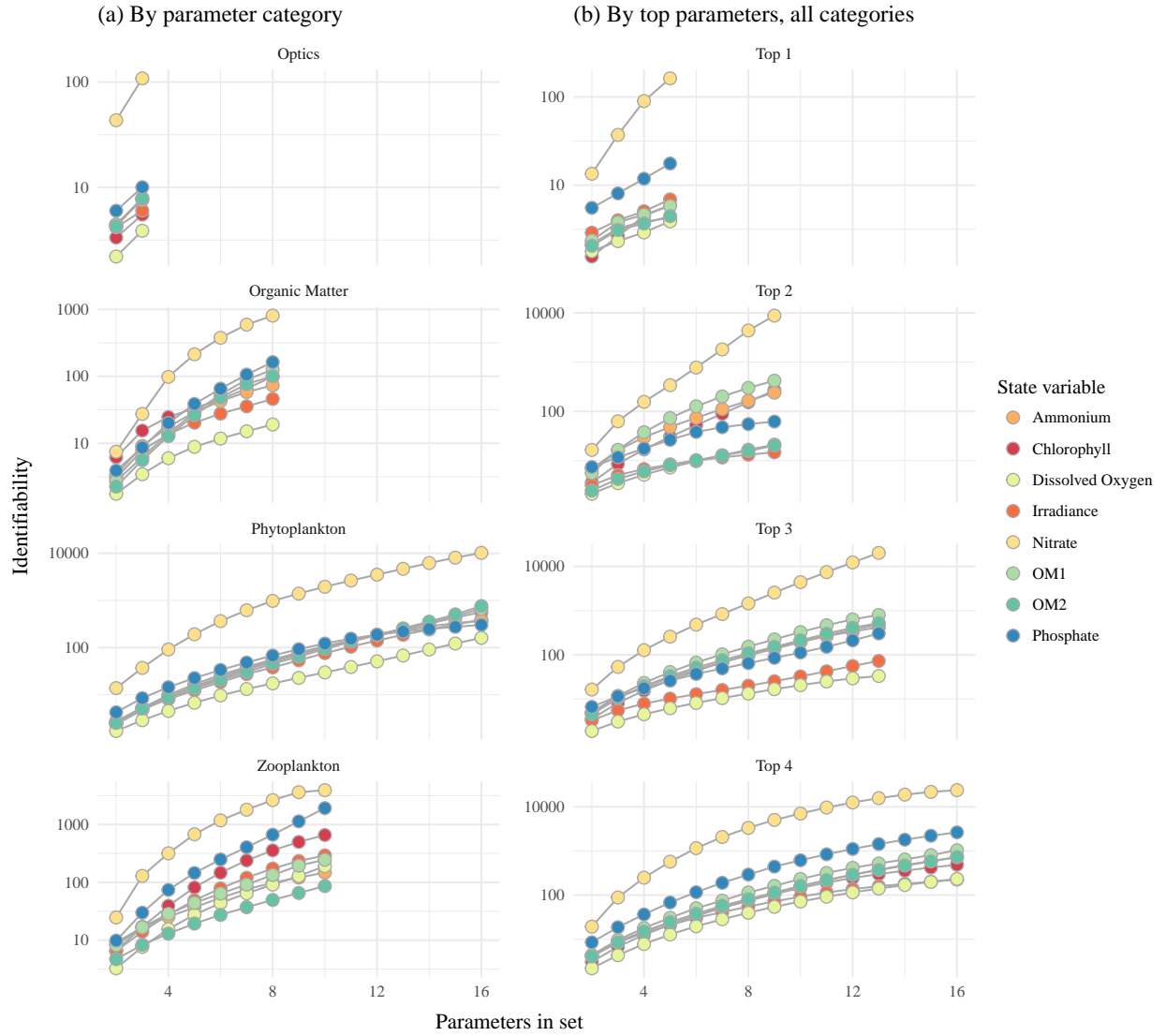
Fig. 4: Average identifiability (as γ, eq. (3)) of parameter subsets for all state variables. Plots in (a) show identifiability by parameter categories and (b) shows identifiability by selecting the top 1 through 4 parameters in all categories. Identifiability was averaged for all combinations in a parameter set to evaluate relative differenes between state variables. The temperature category is not shown because all state variables were sensitive to only one parameter (i.e., $\gamma = 1$, see ??).
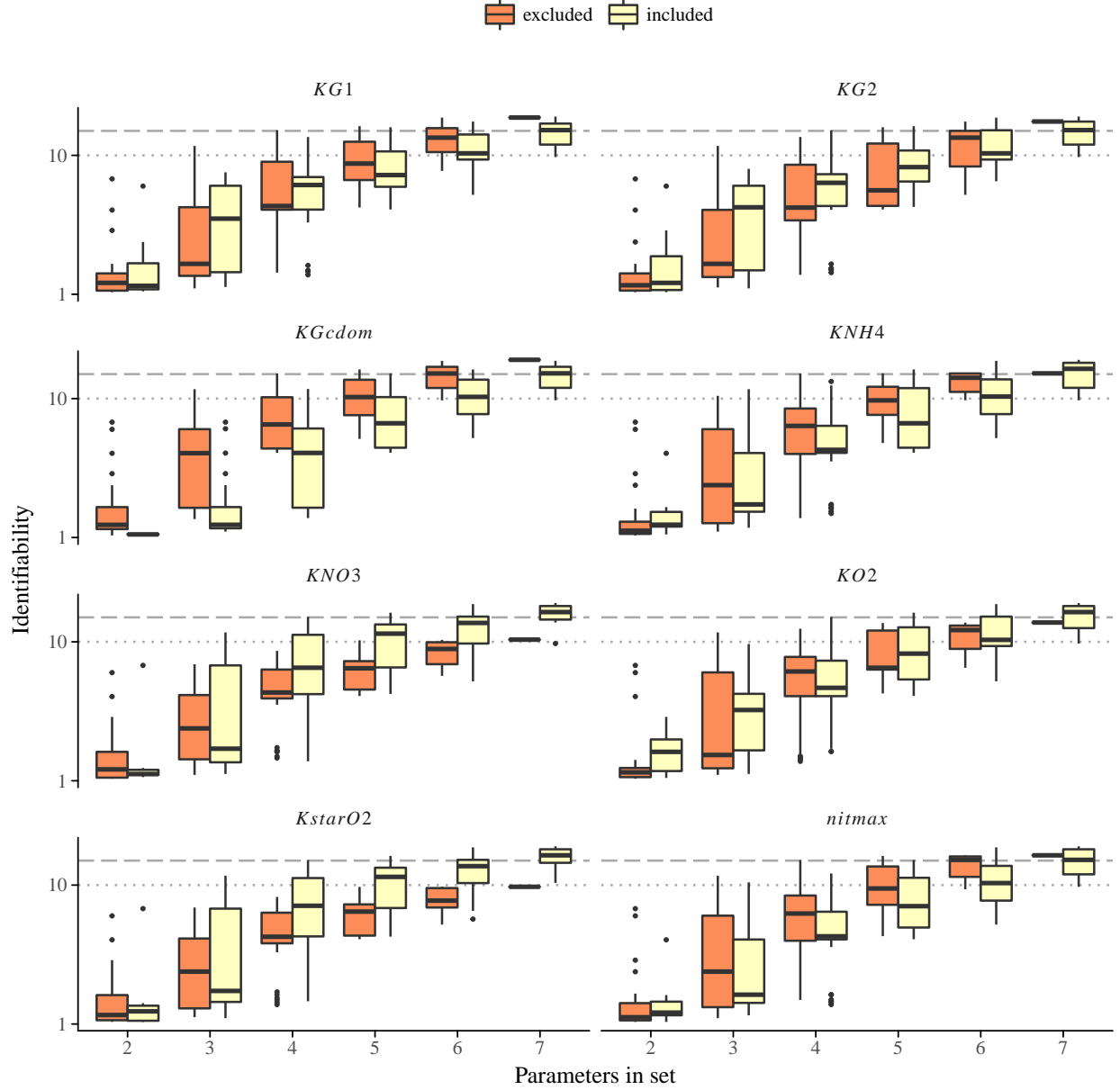
Fig. 5: Identifiability (as γ, eq. (3)) for O_2 of organic matter parameters for subset combinations in Fig. 3. Identifiability is evaluated for subsets that excluded and included the parameters at the top of each plot. Identifiability of including all eight parameters is in Fig. 3. Grey lines indicate potential thresholds at $\gamma = 10, 15$ for maximum acceptable identifiability.
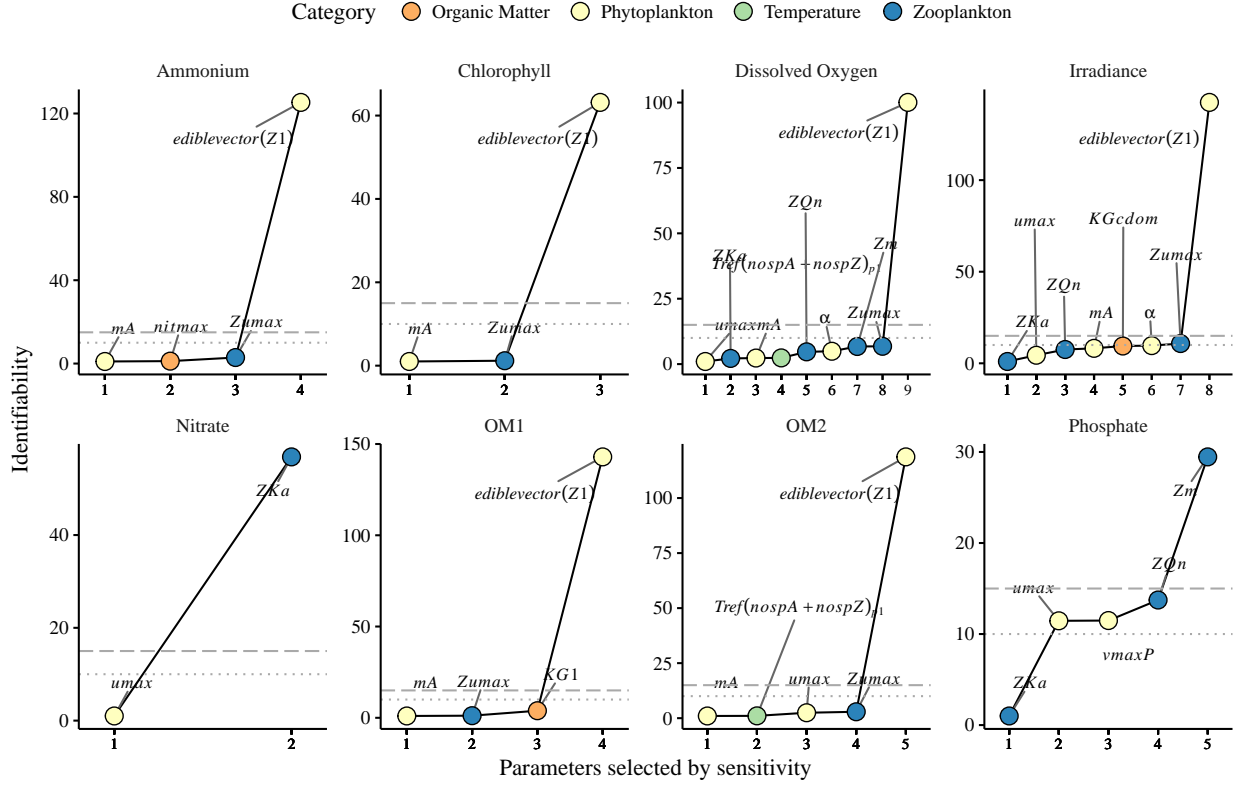
Fig. 6: Identifiability (as γ, eq. (3)) of selecting parameters for all state variables. Parameters are selected by decreasing sensitivity independent of parameter categories. Grey lines indicate potential thresholds at $\gamma = 10, 15$ for maximum acceptable identifiability. Selection stops after $\gamma > 15$.
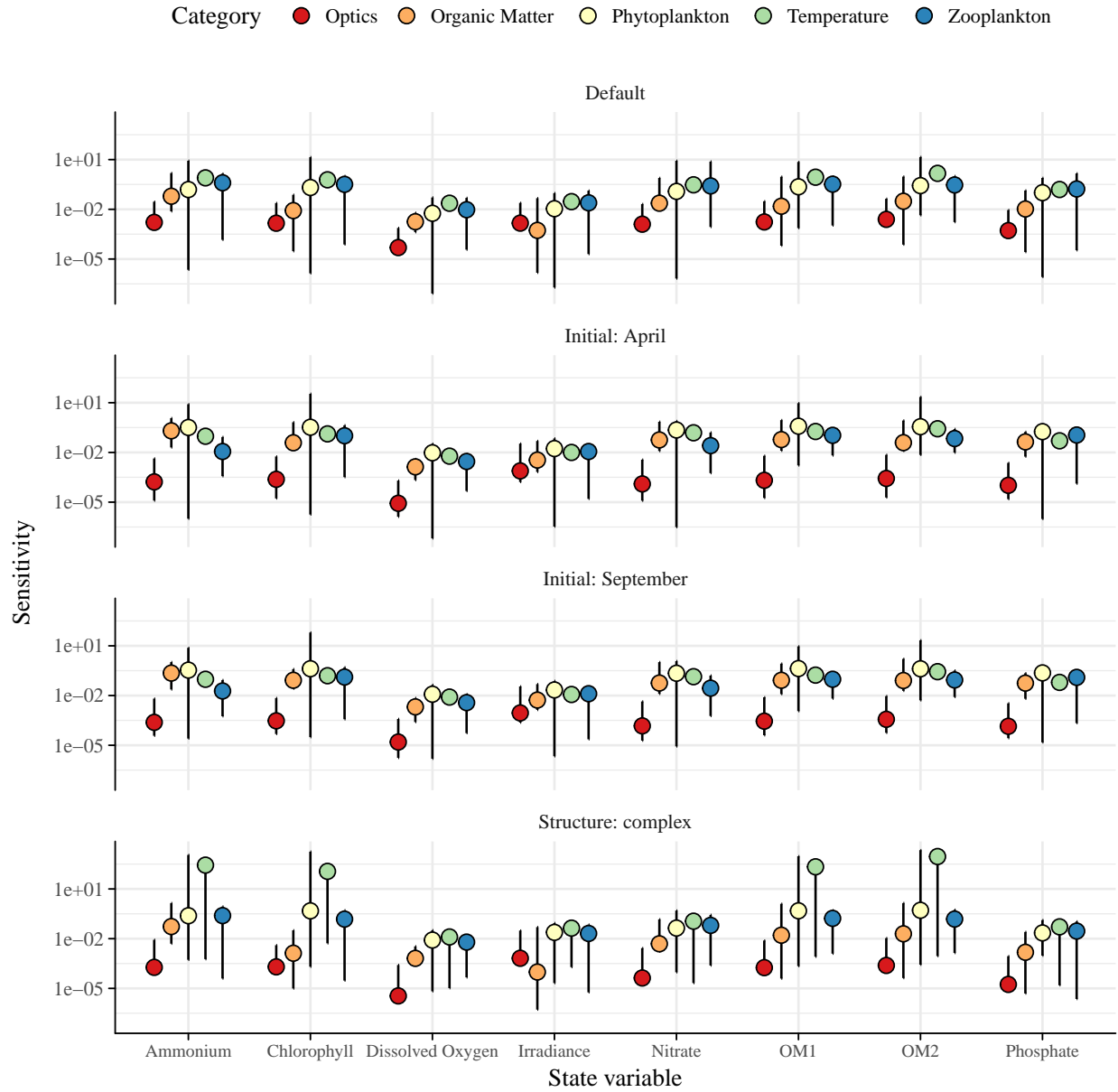
Fig. 7: Summaries of changes in parameter sensitivity values (L1, eq. (2)) from the default model conditions. Sensitivity was re-evaluated using initial conditions as seasonal means for April and September, and added structural complexity. Sensitivity is summarized as the minimum, median, and maximum for each state variable separated by parameter categories. Changes in average sensitivity from the default model conditions are in Table 7.

Table S1: Sensitivity of ammonium to perturbations of individual parameters. Sensitivities are based on a 50% increase from the initial parameter value, where $L1$ summarizes differences in model output from the default (see eq. (2)). Parameters that did not affect ammonium are not shown. Parameters are grouped by categories as optics, temperature, phytoplankton, zooplankton, and organic matter.

Description	Parameter	L1
Optics		
Chla specific absorption at 490 nm	astar490	0.03
OMA specific absorption at 490 nm	astarOMA	1.63×10^{-3}
OMZ specific absorption at 490 nm	astarOMZ	1.5×10^{-3}
Temperature		
Optimum temperature for growth(C)	$Tref(nospA+nospZ)_{p1}$	0.79
Phytoplankton		
mortality coefficient	mA	8.49
edibility vector for Z1	ediblevector(Z1)	1.32
maximum growth rate	umax	0.65
initial slope of the photosynthesis-irradiance relationship	alpha	0.6
N-uptake rate measured at umax	vmaxN	0.46
Phytoplankton threshold for grazing, is multiplied by VOLcell	Athresh	0.29
coefficient for non-limiting nutrient	aN	0.17
phytoplankton growth respiration coefficient	respg	0.16
phytoplankton basal respiration coefficient	respb	0.15
half-saturation constant for P	Kp	0.14
phytoplankton volume/cell	volcell	0.14
minimum N cell-quota	QminN	0.1
P-uptake rate measured at umax	vmaxP	0.1
phytoplankton carbon/cell	Qc	0.03
half-saturation constant for N	Kn	0.01
minimum P cell-quota	QminP	2.24×10^{-6}
Zooplankton		
maximum growth rate of zooplankton	Zumax	1.42
assimilation efficiency as a fraction of ingestion	Zeffic	0.76
half saturation coefficient for grazing	ZKa	0.74
zooplankton nitrogen/individual	ZQn	0.62
Zooplankton mortality constant for quadratic mortality	Zm	0.5
proportion of grazed phytoplankton lost to sloppy feeding	Zslop	0.3
Zooplankton growth-dependent respiration factor	Zrespg	0.22
Zooplankton biomass-dependent respiration factor	Zrespb	0.16
zooplankton phosphorus/individual	ZQp	1.07×10^{-3}
zooplankton carbon/individual	ZQc	1.44×10^{-4}
Organic Matter		
maximum rate of nitrification per day	nitmax	1.54
NH4 rate constant for nitrification	KNH4	0.66
turnover rate for OM1A and OM1Z	KG1	0.07
decay rate of CDOM, 1/day	KGcdom	0.07
half-saturation concentration for O2 utilization	KO2	0.06
O2 concentration that inhibits denitrification	KstarO2	0.05
turnover rate for OM2A and OM2Z	KG2	0.03
half-saturation concentration for NO3 used in denitrification	KNO3	7.55×10^{-3}

Table S2: Sensitivity of chl-*a* to perturbations of individual parameters. Sensitivities are based on a 50% increase from the initial parameter value, where $L1$ summarizes differences in model output from the default (see eq. (2)). Parameters that did not affect chl-*a* are not shown. Parameters are grouped by categories as optics, temperature, phytoplankton, zooplankton, and organic matter.

Description	Parameter	L1
Optics		
Chla specific absorption at 490 nm	*astar490*	0.02
OMA specific absorption at 490 nm	*astarOMA*	1.45×10^{-3}
OMZ specific absorption at 490 nm	*astarOMZ*	1.13×10^{-3}
Temperature		
Optimum temperature for growth(C)	*Tref(nospA+nospZ)$_{p1}$*	0.6
Phytoplankton		
mortality coefficient	*mA*	13.94
edibility vector for Z1	*ediblevector(Z1)*	0.95
maximum growth rate	*umax*	0.85
initial slope of the photosynthesis-irradiance relationship	*alpha*	0.62
N-uptake rate measured at umax	*vmaxN*	0.53
phytoplankton growth respiration coefficient	*respg*	0.26
Phytoplankton threshold for grazing, is multiplied by VOLcell	*Athresh*	0.25
phytoplankton basal respiration coefficient	*respb*	0.24
coefficient for non-limiting nutrient	*aN*	0.17
half-saturation constant for P	*Kp*	0.14
P-uptake rate measured at umax	*vmaxP*	0.12
phytoplankton volume/cell	*volcell*	0.1
minimum N cell-quota	*QminN*	0.07
phytoplankton carbon/cell	*Qc*	0.02
half-saturation constant for N	*Kn*	0.01
minimum P cell-quota	*QminP*	1.38×10^{-6}
Zooplankton		
maximum growth rate of zooplankton	*Zumax*	1.02
half saturation coefficient for grazing	*ZKa*	0.85
assimilation efficiency as a fraction of ingestion	*Zeffic*	0.57
zooplankton nitrogen/individual	*ZQn*	0.52
Zooplankton mortality constant for quadratic mortality	*Zm*	0.41
proportion of grazed phytoplankton lost to sloppy feeding	*Zslop*	0.23
Zooplankton growth-dependent respiration factor	*Zrespg*	0.17
Zooplankton biomass-dependent respiration factor	*Zrespb*	0.14
zooplankton phosphorus/individual	*ZQp*	1.29×10^{-3}
zooplankton carbon/individual	*ZQc*	7.55×10^{-5}
Organic Matter		
decay rate of CDOM, 1/day	*KGcdom*	0.07
turnover rate for OM1A and OM1Z	*KG1*	0.03
turnover rate for OM2A and OM2Z	*KG2*	0.01
O2 concentration that inhibits denitrification	*KstarO2*	0.01
half-saturation concentration for O2 utilization	*KO2*	3.35×10^{-3}
half-saturation concentration for NO3 used in denitrification	*KNO3*	1.19×10^{-3}
maximum rate of nitrification per day	*nitmax*	3.4×10^{-5}
NH4 rate constant for nitrification	*KNH4*	2.97×10^{-5}

Table S3: Sensitivity of irradiance to perturbations of individual parameters. Sensitivities are based on a 50% increase from the initial parameter value, where $L1$ summarizes differences in model output from the default (see eq. (2)). Parameters that did not affect irradiance are not shown. Parameters are grouped by categories as optics, temperature, phytoplankton, zooplankton, and organic matter.

Description	Parameter	L1
Optics		
Chla specific absorption at 490 nm	*astar490*	0.02
OMA specific absorption at 490 nm	*astarOMA*	1.47×10^{-3}
OMZ specific absorption at 490 nm	*astarOMZ*	1.34×10^{-3}
Temperature		
Optimum temperature for growth(C)	*Tref(nospA+nospZ)$_{p1}$*	0.03
Phytoplankton		
maximum growth rate	*umax*	0.09
mortality coefficient	*mA*	0.05
initial slope of the photosynthesis-irradiance relationship	*alpha*	0.04
edibility vector for Z1	*ediblevector(Z1)*	0.04
N-uptake rate measured at umax	*vmaxN*	0.03
Phytoplankton threshold for grazing, is multiplied by VOLcell	*Athresh*	0.02
coefficient for non-limiting nutrient	*aN*	0.01
phytoplankton growth respiration coefficient	*respg*	0.01
half-saturation constant for P	*Kp*	0.01
P-uptake rate measured at umax	*vmaxP*	9.48×10^{-3}
phytoplankton basal respiration coefficient	*respb*	9.38×10^{-3}
phytoplankton volume/cell	*volcell*	8.1×10^{-3}
minimum N cell-quota	*QminN*	5.75×10^{-3}
phytoplankton carbon/cell	*Qc*	3.78×10^{-3}
half-saturation constant for N	*Kn*	9.81×10^{-4}
minimum P cell-quota	*QminP*	1.92×10^{-7}
Zooplankton		
half saturation coefficient for grazing	*ZKa*	0.13
zooplankton nitrogen/individual	*ZQn*	0.06
maximum growth rate of zooplankton	*Zumax*	0.04
Zooplankton mortality constant for quadratic mortality	*Zm*	0.04
assimilation efficiency as a fraction of ingestion	*Zeffic*	0.03
proportion of grazed phytoplankton lost to sloppy feeding	*Zslop*	0.02
Zooplankton growth-dependent respiration factor	*Zrespg*	0.01
Zooplankton biomass-dependent respiration factor	*Zrespb*	9.67×10^{-3}
zooplankton phosphorus/individual	*ZQp*	9.34×10^{-5}
zooplankton carbon/individual	*ZQc*	1.99×10^{-5}
Organic Matter		
decay rate of CDOM, 1/day	*KGcdom*	0.05
turnover rate for OM1A and OM1Z	*KG1*	3.96×10^{-3}
turnover rate for OM2A and OM2Z	*KG2*	9.88×10^{-4}
O2 concentration that inhibits denitrification	*KstarO2*	7.2×10^{-4}
half-saturation concentration for O2 utilization	*KO2*	3.54×10^{-4}
half-saturation concentration for NO3 used in denitrification	*KNO3*	6.18×10^{-5}
maximum rate of nitrification per day	*nitmax*	1.72×10^{-6}
NH4 rate constant for nitrification	*KNH4*	1.48×10^{-6}

Table S4: Sensitivity of nitrate to perturbations of individual parameters. Sensitivities are based on a 50% increase from the initial parameter value, where $L1$ summarizes differences in model output from the default (see eq. (2)). Parameters that did not affect nitrate are not shown. Parameters are grouped by categories as optics, temperature, phytoplankton, zooplankton, and organic matter.

Description	Parameter	L1
Optics		
Chla specific absorption at 490 nm	astar490	0.02
OMZ specific absorption at 490 nm	astarOMZ	1.27×10^{-3}
OMA specific absorption at 490 nm	astarOMA	1.19×10^{-3}
Temperature		
Optimum temperature for growth(C)	$Tref(nospA+nospZ)_{p1}$	0.3
Phytoplankton		
maximum growth rate	umax	8.49
phytoplankton carbon/cell	Qc	0.89
initial slope of the photosynthesis-irradiance relationship	alpha	0.7
edibility vector for Z1	ediblevector(Z1)	0.33
mortality coefficient	mA	0.27
Phytoplankton threshold for grazing, is multiplied by VOLcell	Athresh	0.2
N-uptake rate measured at umax	vmaxN	0.19
coefficient for non-limiting nutrient	aN	0.13
phytoplankton growth respiration coefficient	respg	0.11
phytoplankton volume/cell	volcell	0.1
P-uptake rate measured at umax	vmaxP	0.1
half-saturation constant for P	Kp	0.09
minimum N cell-quota	QminN	0.09
phytoplankton basal respiration coefficient	respb	0.07
half-saturation constant for N	Kn	7.06×10^{-3}
minimum P cell-quota	QminP	6.67×10^{-7}
Zooplankton		
half saturation coefficient for grazing	ZKa	7.59
zooplankton nitrogen/individual	ZQn	1.17
Zooplankton mortality constant for quadratic mortality	Zm	0.7
maximum growth rate of zooplankton	Zumax	0.34
proportion of grazed phytoplankton lost to sloppy feeding	Zslop	0.26
assimilation efficiency as a fraction of ingestion	Zeffic	0.25
Zooplankton growth-dependent respiration factor	Zrespg	0.17
Zooplankton biomass-dependent respiration factor	Zrespb	0.1
zooplankton carbon/individual	ZQc	3.8×10^{-3}
zooplankton phosphorus/individual	ZQp	8.59×10^{-4}
Organic Matter		
O2 concentration that inhibits denitrification	KstarO2	0.78
half-saturation concentration for NO3 used in denitrification	KNO3	0.07
decay rate of CDOM, 1/day	KGcdom	0.04
half-saturation concentration for O2 utilization	KO2	0.03
turnover rate for OM1A and OM1Z	KG1	0.02
turnover rate for OM2A and OM2Z	KG2	0.01
maximum rate of nitrification per day	nitmax	9.96×10^{-3}
NH4 rate constant for nitrification	KNH4	9.87×10^{-3}

Table S5: Sensitivity of particulate organic matter to perturbations of individual parameters. Sensitivities are based on a 50% increase from the initial parameter value, where $L1$ summarizes differences in model output from the default (see eq. (2)). Parameters that did not affect particulate organic matter are not shown. Parameters are grouped by categories as optics, temperature, phytoplankton, zooplankton, and organic matter.

Description	Parameter	L1
Optics		
Chla specific absorption at 490 nm	astar490	0.03
OMA specific absorption at 490 nm	astarOMA	1.73×10^{-3}
OMZ specific absorption at 490 nm	astarOMZ	1.49×10^{-3}
Temperature		
Optimum temperature for growth(C)	$Tref(nospA+nospZ)_{p1}$	0.86
Phytoplankton		
mortality coefficient	mA	7.22
edibility vector for Z1	ediblevector(Z1)	0.9
maximum growth rate	umax	0.89
phytoplankton carbon/cell	Qc	0.67
initial slope of the photosynthesis-irradiance relationship	alpha	0.67
N-uptake rate measured at umax	vmaxN	0.45
phytoplankton growth respiration coefficient	respg	0.29
phytoplankton basal respiration coefficient	respb	0.24
Phytoplankton threshold for grazing, is multiplied by VOLcell	Athresh	0.22
minimum N cell-quota	QminN	0.21
coefficient for non-limiting nutrient	aN	0.14
half-saturation constant for P	Kp	0.11
phytoplankton volume/cell	volcell	0.1
P-uptake rate measured at umax	vmaxP	0.09
half-saturation constant for N	Kn	0.01
minimum P cell-quota	QminP	7.35×10^{-4}
Zooplankton		
maximum growth rate of zooplankton	Zumax	0.96
half saturation coefficient for grazing	ZKa	0.79
assimilation efficiency as a fraction of ingestion	Zeffic	0.54
zooplankton nitrogen/individual	ZQn	0.49
Zooplankton mortality constant for quadratic mortality	Zm	0.39
proportion of grazed phytoplankton lost to sloppy feeding	Zslop	0.27
Zooplankton growth-dependent respiration factor	Zrespg	0.16
Zooplankton biomass-dependent respiration factor	Zrespb	0.12
zooplankton carbon/individual	ZQc	9.64×10^{-3}
zooplankton phosphorus/individual	ZQp	1.06×10^{-3}
Organic Matter		
turnover rate for OM1A and OM1Z	KG1	0.92
decay rate of CDOM, 1/day	KGcdom	0.07
half-saturation concentration for O2 utilization	KO2	0.04
O2 concentration that inhibits denitrification	KstarO2	0.02
turnover rate for OM2A and OM2Z	KG2	0.01
half-saturation concentration for NO3 used in denitrification	KNO3	3.72×10^{-3}
maximum rate of nitrification per day	nitmax	6.98×10^{-5}
NH4 rate constant for nitrification	KNH4	6.41×10^{-5}

Table S6: Sensitivity of dissolved organic matter to perturbations of individual parameters. Sensitivities are based on a 50% increase from the initial parameter value, where $L1$ summarizes differences in model output from the default (see eq. (2)). Parameters that did not affect dissolved organic matter are not shown. Parameters are grouped by categories as optics, temperature, phytoplankton, zooplankton, and organic matter.

Description	Parameter	L1
Optics		
Chla specific absorption at 490 nm	*astar490*	0.04
OMA specific absorption at 490 nm	*astarOMA*	2.48×10^{-3}
OMZ specific absorption at 490 nm	*astarOMZ*	2.04×10^{-3}
Temperature		
Optimum temperature for growth(C)	*Tref(nospA+nospZ)$_{p1}$*	1.48
Phytoplankton		
mortality coefficient	*mA*	14.25
maximum growth rate	*umax*	1.11
edibility vector for Z1	*ediblevector(Z1)*	0.94
N-uptake rate measured at umax	*vmaxN*	0.86
initial slope of the photosynthesis-irradiance relationship	*alpha*	0.85
phytoplankton carbon/cell	*Qc*	0.67
phytoplankton growth respiration coefficient	*respg*	0.36
phytoplankton basal respiration coefficient	*respb*	0.29
coefficient for non-limiting nutrient	*aN*	0.25
minimum N cell-quota	*QminN*	0.24
Phytoplankton threshold for grazing, is multiplied by VOLcell	*Athresh*	0.22
half-saturation constant for P	*Kp*	0.2
P-uptake rate measured at umax	*vmaxP*	0.14
phytoplankton volume/cell	*volcell*	0.1
half-saturation constant for N	*Kn*	0.02
minimum P cell-quota	*QminP*	4.37×10^{-3}
Zooplankton		
maximum growth rate of zooplankton	*Zumax*	1.01
half saturation coefficient for grazing	*ZKa*	0.88
assimilation efficiency as a fraction of ingestion	*Zeffic*	0.58
zooplankton nitrogen/individual	*ZQn*	0.54
Zooplankton mortality constant for quadratic mortality	*Zm*	0.41
Zooplankton growth-dependent respiration factor	*Zrespg*	0.17
Zooplankton biomass-dependent respiration factor	*Zrespb*	0.13
proportion of grazed phytoplankton lost to sloppy feeding	*Zslop*	0.12
zooplankton carbon/individual	*ZQc*	0.04
zooplankton phosphorus/individual	*ZQp*	1.69×10^{-3}
Organic Matter		
turnover rate for OM2A and OM2Z	*KG2*	0.94
decay rate of CDOM, 1/day	*KGcdom*	0.1
half-saturation concentration for O2 utilization	*KO2*	0.04
turnover rate for OM1A and OM1Z	*KG1*	0.04
O2 concentration that inhibits denitrification	*KstarO2*	0.03
half-saturation concentration for NO3 used in denitrification	*KNO3*	3.16×10^{-3}
maximum rate of nitrification per day	*nitmax*	8.44×10^{-5}
NH4 rate constant for nitrification	*KNH4*	7.41×10^{-5}

Table S7: Sensitivity of phosphate to perturbations of individual parameters. Sensitivities are based on a 50% increase from the initial parameter value, where $L1$ summarizes differences in model output from the default (see eq. (2)). Parameters that did not affect phosphate are not shown. Parameters are grouped by categories as optics, temperature, phytoplankton, zooplankton, and organic matter.

Description	Parameter	L1
Optics		
Chla specific absorption at 490 nm	*astar490*	9.01×10^{-3}
OMZ specific absorption at 490 nm	*astarOMZ*	5.21×10^{-4}
OMA specific absorption at 490 nm	*astarOMA*	5.13×10^{-4}
Temperature		
Optimum temperature for growth(C)	*Tref(nospA+nospZ)$_{p1}$*	0.16
Phytoplankton		
maximum growth rate	*umax*	0.78
P-uptake rate measured at umax	*vmaxP*	0.59
edibility vector for Z1	*ediblevector(Z1)*	0.25
initial slope of the photosynthesis-irradiance relationship	*alpha*	0.23
mortality coefficient	*mA*	0.2
N-uptake rate measured at umax	*vmaxN*	0.18
Phytoplankton threshold for grazing, is multiplied by VOLcell	*Athresh*	0.13
coefficient for non-limiting nutrient	*aN*	0.11
phytoplankton growth respiration coefficient	*respg*	0.09
phytoplankton volume/cell	*volcell*	0.06
phytoplankton basal respiration coefficient	*respb*	0.06
minimum N cell-quota	*QminN*	0.04
half-saturation constant for P	*Kp*	0.03
half-saturation constant for N	*Kn*	6.97×10^{-3}
phytoplankton carbon/cell	*Qc*	6.68×10^{-3}
minimum P cell-quota	*QminP*	8.21×10^{-7}
Zooplankton		
half saturation coefficient for grazing	*ZKa*	1.47
zooplankton nitrogen/individual	*ZQn*	0.5
Zooplankton mortality constant for quadratic mortality	*Zm*	0.35
maximum growth rate of zooplankton	*Zumax*	0.26
assimilation efficiency as a fraction of ingestion	*Zeffic*	0.19
proportion of grazed phytoplankton lost to sloppy feeding	*Zslop*	0.15
Zooplankton growth-dependent respiration factor	*Zrespg*	0.1
Zooplankton biomass-dependent respiration factor	*Zrespb*	0.06
zooplankton phosphorus/individual	*ZQp*	6.43×10^{-3}
zooplankton carbon/individual	*ZQc*	3.38×10^{-5}
Organic Matter		
turnover rate for OM1A and OM1Z	*KG1*	0.14
turnover rate for OM2A and OM2Z	*KG2*	0.06
decay rate of CDOM, 1/day	*KGcdom*	0.02
half-saturation concentration for O2 utilization	*KO2*	0.01
O2 concentration that inhibits denitrification	*KstarO2*	7.29×10^{-3}
half-saturation concentration for NO3 used in denitrification	*KNO3*	1.19×10^{-3}
maximum rate of nitrification per day	*nitmax*	2.7×10^{-5}
NH4 rate constant for nitrification	*KNH4*	2.64×10^{-5}